CZECH TECHNICAL UNIVERSITY IN PRAGUE
FACULTY OF MECHANICAL ENGINEERING

DOCTORAL THESIS STATEMENT

Czech Technical University in Prague
Faculty of Mechanical Engineering
Department of Technical Mathematics

Doctoral thesis statement

NUMERICAL SOLUTION OF TURBULENT FLOW USING DES MODEL WITH MESH ADAPTATION

Ing. Lukáš Hájek

Doctoral study programme: Mechanical Engineering

Branch of study: Mathematical and Physical Engineering

Supervisor: prof. Ing. Jaroslav Fořt, CSc.

Co-supervisor: Ing. Jan Karel, Ph.D.

A doctoral thesis statement submitted for the degree of “Doctor”, abbreviated to “Ph.D.”

Prague, 2023

The doctoral thesis was produced during a Ph.D. study in a combined form at the Department of Technical Mathematics of the Faculty of Mechanical Engineering of the Czech Technical University in Prague.

Candidate:	Ing. Lukáš Hájek Department of Technical Mathematics, Faculty of Mechanical Engineering, CTU in Prague Karlovo náměstí 13, 121 35 Prague 2
Supervisor:	prof. Ing. Jaroslav Fořt, CSc. Department of Technical Mathematics, Faculty of Mechanical Engineering, CTU in Prague Karlovo náměstí 13, 121 35 Prague 2
Co-supervisor:	Ing. Jan Karel, Ph.D. Department of Technical Mathematics, Faculty of Mechanical Engineering, CTU in Prague Karlovo náměstí 13, 121 35 Prague 2
Opponents:	

The doctoral thesis statement was distributed on: ....

The defence of the doctoral thesis will be held on .... at .... a.m./p.m. before the Board for the Defence of the Doctoral Thesis in the branch of study Mathematical and Physical Engineering in the meeting room No. .... of the Faculty of Mechanical Engineering of the CTU in Prague.

Those interested may get acquainted with the doctoral thesis concerned at the Department for Science and Research of the Faculty of Mechanical Engineering of the CTU in Prague, Technická 4, Prague 6.

Prof. Ing. Jiří Fürst, Ph.D.
Chairman of the Board for the Defence of the Doctoral Thesis in the branch of study
Mathematical and Physical Engineering
Faculty of Mechanical Engineering, CTU in Prague

Contents

Nomenclature

β	Turbulence model constant	[1]
β^*	Turbulence model constant	[1]
γ	Ratio of specific heats	[1]
$\boldsymbol{\sigma}$	Viscous stress tensor	[Pa]
$\boldsymbol{\tau}$	Reynolds stress tensor	[Pa]
$\boldsymbol{S}$	Strain-rate tensor	[Hz]
$\boldsymbol{u}$	Fluid velocity vector with components u_1, u_2, u_3	[$\mathrm{m\,s^{-1}}$]
$\mathbb{1}$	Identity matrix	[1]
μ	Dynamic viscosity	[Pa s]
μ_T	Dynamic eddy viscosity	[Pa s]
ν_T	Kinematic eddy viscosity	[$\mathrm{m^2\,s^{-1}}$]
ω	Specific turbulence dissipation rate	[$\mathrm{s^{-1}}$]
ρ	Fluid density	[$\mathrm{kg\,m^{-3}}$]
σ_k	Turbulence model constant	[1]
$\sigma_{\omega 2}$	Turbulence model constant	[1]
σ_ω	Turbulence model constant	[1]
Pr	Prandtl number	[1]
Pr_T	Turbulent Prandtl number	[1]
θ	Angle describing the surface of a given cylinder	[°]
C_D	Cross-diffusion term	[$\mathrm{kg\,m^{-3}\,s^{-2}}$]
c_p	Specific heat capacity at constant pressure	[$\mathrm{J\,kg^{-1}\,K^{-1}}$]
c_V	Specific heat capacity at constant volume	[$\mathrm{J\,kg^{-1}\,K^{-1}}$]
C_ω	Turbulence model constant	[1]
d_w	Distance to the nearest wall	[m]
E	Specific energy	[$\mathrm{J\,kg^{-1}}$]
$F_{1,2}$	Blending functions for the SST turbulence model	[1]
H	Specific enthalpy	[$\mathrm{J\,kg^{-1}}$]
k	Turbulence kinetic energy	[$\mathrm{J\,kg^{-1}}$]
L_T	Model length scale	[m]
p	Pressure	[Pa]
P_k	Production of turbulence kinetic energy	[$\mathrm{J\,m^{-3}\,s^{-1}}$]
P_ω	Production of specific turbulence dissipation rate	[$\mathrm{kg\,m^{-3}\,s^{-2}}$]
R	Specific gas constant	[$\mathrm{J\,kg^{-1}\,K^{-1}}$]
S	Norm of the strain-rate tensor	[Hz]
T	Temperature	[K]
t	Time	[s]

1 Introduction

Motivation. Fluid mechanics is important for a whole range of fields such as engineering, chemistry and meteorology. Computational fluid dynamics (CFD) deals with the problem of resolving flows of these fluids. One of the more difficult but important aspects of fluid mechanics is turbulent flow.

There are various approaches to turbulence modeling such as direct numerical simulation (DNS) of Navier–Stokes equations, large eddy simulation (LES) or Reynolds-averaged Navier–Stokes (RANS) equations. While DNS is too costly for most applications, LES can provide a suitable alternative able to resolve wide range of turbulence length scales. However, LES can still be too demanding for certain applications, requiring high resolution of computational meshes, which becomes most significant around walls. On the other hand, modeling turbulence with RANS approach can work with lower resolution computational grids, but the cost is the inability to resolve all turbulent scales properly.

RANS-LES hybrid methods are aimed at providing the best of both worlds, utilizing RANS in the regions around walls and LES further away from these areas to resolve detached eddies. The switching between the two approaches can be done in various ways, several of which are employed in the thesis, along with two newly proposed methods.

As LES models require high resolution of computational meshes, LES mode of RANS-LES hybrid methods has similar demands and is only employed in regions where the grid cells are small enough. This can be influenced by adaptive mesh refinement (AMR), increasing mesh resolution on the fly when needed. The thesis also proposes a number of ways how to combine the hybrid methods with AMR.

All the results presented in the thesis were computed using the in-house parallel numerical software Orion. Its code has been developed partly as a part of the thesis and partly by the rest of the Orion team, namely Prof. Jaroslav Fořt, Dr. Jan Karel, Dr. Matěj Klíma, and Dr. David Trdlička.

State of the art. RANS-LES hybrid methods are relatively young family of turbulence models – the first hybrid method was probably the detached eddy simulation (DES) model proposed by Spalart et al. in 1997 [4]. It was emphasized by Menter and Kuntz in 2004 [5] (among others) that grid spacing can negatively affect results of DES and lead to a so-called modeled-stress depletion (MSD). Spalart et. al in 2006 proposed solution to this problem in [6] with the delayed detached eddy simulation (DDES) model, using a blending function and making the RANS-LES switching non-binary. The article also discusses issues with velocity profiles near walls because of the effects described by Nikitin et al. in [7], known as log-layer mismatch, which was later solved by Shur et al. in 2008 [8], which combined the DDES approach with wall-modeled LES (WMLES) and gave birth to the first improved DDES (IDDES) model.

In 2001, Strelets [9] proposed a version of DES using the Menter's Shear Stress Transport (SST) RANS model from 1993 [10], instead of the commonly used SA model.

Both DDES and IDDES hybrid models based on the SST model were later proposed by Gritskevich et al. in 2011 [11]. These models are also used in the thesis.

Another DES method was proposed by Kok in 2004 [12], named Extra-Large Eddy Simulation (X-LES) and based on Kok's TNT model from 2000 [13], later modified with a stochastic term to improve the development of turbulent free shear layers, which led to his introduction of a stochastic variant of the X-LES model in 2009 [14]. In the thesis, the TNT model and the stochastic variant of the X-LES method are used.

The DDES and IDDES versions of the X-LES model never came into being, with one possible exception of the Delayed X-LES model by Fracassi et al. from 2022 [15], however, the authors of this method replaced the base RANS TNT model with SST. Therefore, the TNT-based Delayed X-LES (DX-LES) and Improved DX-LES (IDX-LES) models are newly proposed in the thesis.

Adaptive mesh refinement has also been very rarely used with hybrid methods, despite its great potential for this combination. One of the few examples can be a very recent article by Mazaffari from 2022 [16], which only introduces the mesh adaptation based on time-averaged quantities. Therefore, in the thesis, the problem of tandem cylinders is also solved by the DES method with mesh adaptation.

Aims of the work. The main aim of the thesis is the description, implementation and testing of various hybrid detached eddy simulation methods and their delayed variants. Adaptive mesh refinement should then be added to these methods. Overall, the objectives of the thesis are:

- implement the HLLC scheme with analytic Jacobians in the implicit parallel in-house code Orion,
- describe and implement the RANS-LES hybrid models X-LES [12] (based on the TNT method), SST-DES [9], DDES and IDDES [11] (based on the SST method) in the implicit formulation,
- derive new versions of the X-LES model with non-binary switching using the blending introduces in SST-DDES and SST-IDDES, then describe and implement it similarly to the previous hybrid methods,
- use the 2D algorithm of adaptive mesh refinement from [17] already implemented in Orion and extend it for 3D grids with several identical layers, propose several adaptation criteria to detect turbulent phenomena,
- test and compare the implemented RANS and hybrid RANS-LES methods (and the effect of their switches) as well as different adaptation criteria,
- show the effect of adaptive mesh refinement on the results of a RANS-LES hybrid method.

2 Mathematical model

RANS Equations for implementing turbulence models. Using Fourier's law of heat conduction and its Reynolds analogy to obtain an approximation of the turbulent heat flux and using generally the same assumptions as [18], the Reynolds-averaged Navier–Stokes equations can be written as

$$\frac{\partial \rho}{\partial t} + \operatorname{div}(\rho \boldsymbol{u}) = 0, \tag{1a}$$

$$\frac{\partial \rho \boldsymbol{u}}{\partial t} + \operatorname{div}((\rho \boldsymbol{u}) \otimes \boldsymbol{u}) = \operatorname{div} \boldsymbol{\sigma} + \operatorname{div} \boldsymbol{\tau} - \operatorname{grad} p, \tag{1b}$$

$$\begin{aligned}\frac{\partial \rho E}{\partial t} + \operatorname{div}(\rho \boldsymbol{u} H) &= \operatorname{div}(\boldsymbol{\tau} \boldsymbol{u}) + \operatorname{div}\left(\frac{c_p \mu}{\mathrm{Pr}} \operatorname{grad} T\right) + \operatorname{div}(\boldsymbol{\sigma} \boldsymbol{u}) \\ &+ \operatorname{div}\left(\left[\mu + \frac{\mu_T}{\sigma_k}\right] \operatorname{grad} k + \frac{c_p \mu_T}{\mathrm{Pr}_T} \operatorname{grad} T\right),\end{aligned} \tag{1c}$$

where $\otimes$ denotes outer product, ρ is fluid density, t represents time, $\boldsymbol{u}$ is fluid velocity with u_1, u_2, u_3 as its components, p denotes pressure, E represents specific energy, H is specific enthalpy. The terms from the Fourier's law of heat conduction and its analogy for the turbulent momentum are the temperature T, heat capacity at constant pressure c_p (and the heat capacity at constant volume would be c_V), Prandtl number Pr and its turbulent counterpart Pr_T, dynamic viscosity μ and eddy viscosity μ_T, σ_k is then a coefficient described by a turbulence model for the turbulence kinetic energy k, $\boldsymbol{\sigma}$ represents viscous stress tensor, μ denotes dynamic viscosity, $\boldsymbol{S}$ is strain tensor and $\boldsymbol{\tau}$ is the Reynolds stress tensor obtained by Boussinesq approximation.

We also need the equation of state, which we use the one for the ideal gas. Also, the dynamic viscosity μ of the ideal gas can be approximated through the use of Sutherland's Law. However, even the system of equations (1) expanded by the equation of state is not complete, as it has more unknowns than equations. To fully close the system and obtain the eddy viscosity μ_T, we will need the turbulence model described below.

Turbulence models. As described, we need a turbulence model to obtain the eddy viscosity. All the turbulence models used in the thesis are based on two RANS models: Menter's Shear Stress Transport (SST) [19] and Kok's Turbulent/Non-Turbulent (TNT) [13]. Both of these are two equation turbulence models, where our unknowns are the turbulent kinetic energy k and the specific turbulence dissipation rate ω (and the conservative variables are ρk and $\rho\omega$). These models are commonly referred to simply as "k–ω models".

The equations of the SST-based models can be written as

$$\frac{\partial \rho k}{\partial t} + \operatorname{div}(\rho k \boldsymbol{u}) = \operatorname{div}([\mu + \sigma_k \mu_T] \operatorname{grad} k) + P_k - \rho k \frac{\sqrt{k}}{L_T}, \tag{2a}$$

$$\begin{aligned}\frac{\partial \rho \omega}{\partial t} + \operatorname{div}(\rho \omega \boldsymbol{u}) &= \operatorname{div}([\mu + \sigma_\omega \mu_T] \operatorname{grad} \omega) \\ &+ P_\omega - \beta \rho \omega^2 + 2(1 - F_1)\mathrm{CD},\end{aligned} \tag{2b}$$

where L_T represents the model length scale (which is the only parameter that differs between the models listed in the thesis), P_k and P_ω are the production terms, CD is the diffusion, S is the strain tensor norm $S = \sqrt{2\boldsymbol{S}^2}$, F_1 and F_2 are the SST blending functions described in [19] and d_w is the distance to the nearest wall. Model coefficients σ_k, σ_ω, β, C_ω are described in [19]. The eddy viscosity is then given by:

$$\mu_T^{(\mathrm{SST})} = \frac{a_1 \rho k}{\max\left(a_1 \omega, F_2 S\right)}, \quad a_1 = 0.31. \tag{3}$$

The equations for the TNT-based models can be written as

$$\frac{\partial \rho k}{\partial t} + \operatorname{div}\left(\rho k \boldsymbol{u}\right) = \operatorname{div}\left(\left[\mu + \sigma_k \mu_T\right] \operatorname{grad} k\right) + P_k - \rho k \frac{\sqrt{k}}{L_T}, \tag{4a}$$

$$\frac{\partial \rho \omega}{\partial t} + \operatorname{div}\left(\rho \omega \boldsymbol{u}\right) = \operatorname{div}\left(\left[\mu + \sigma_\omega \mu_T\right] \operatorname{grad} \omega\right) + P_\omega - \beta \rho \omega^2 + C_D, \tag{4b}$$

where, once again, L_T is the model length scale, P_k and P_ω are the production terms and C_D represents the cross-diffusion term. Finally, σ_k, σ_ω, σ_d, α_ω, β. Finally, the eddy viscosity for the TNT-based models is dependent on the model length scale:

$$\mu_T^{(\mathrm{TNT})} = \beta^* \rho \sqrt{k} L_T, \quad \beta^* = 0.09. \tag{5}$$

The model scales are given by:

$$l_{\mathrm{RANS}} = \frac{\sqrt{k}}{\beta^* \omega}, \quad l_{\mathrm{LES}} = C_{\mathrm{DES}} \mathit{\Delta}, \quad \tilde{l}_{\mathrm{LES}} = C_{\mathrm{DES}} \tilde{\mathit{\Delta}}, \quad \hat{l}_{\mathrm{LES}} = C_{\mathrm{DES}} \hat{\mathit{\Delta}}, \tag{6}$$

where where $\mathit{\Delta}$ denotes the maximum length of the cell's edges, $\tilde{\mathit{\Delta}}$ is the cubic root of a given cell and $\hat{\mathit{\Delta}} = \min\left\{C_w \max\left[d_w, \mathit{\Delta}\right], \mathit{\Delta}\right\}$, $C_w = 0.15$.

For the SST-based models, the model length scales for the base RANS SST method and the hybrid DES, DDES and IDDES models are:

$$\begin{aligned} L_T^{(\mathrm{SST})} &= l_{\mathrm{RANS}}, \quad L_T^{(\mathrm{DES})} = \min\left(l_{\mathrm{RANS}}, l_{\mathrm{LES}}\right), \\ L_T^{(\mathrm{DDES})} &= l_{\mathrm{RANS}} - f_d \max\left(0, l_{\mathrm{RANS}} - l_{\mathrm{LES}}\right), \\ L_T^{(\mathrm{IDDES})} &= \tilde{f}_d \left(1 + f_e\right) l_{\mathrm{RANS}} + \left(1 - \tilde{f}_d\right) \hat{l}_{\mathrm{LES}}, \end{aligned}$$

where f_d, $\tilde{f}_d$ and f_d are functions described in [11].

For the TNT-based models, we similarly define the model length scales for the base RANS TNT method, X-LES and the newly proposed delayed and improved delayed X-LES models (DX-LES and IDX-LES):

$$\begin{aligned} L_T^{(\mathrm{TNT})} &= l_{\mathrm{RANS}}, \quad L_T^{(\mathrm{X\text{-}LES})} = \min\left(l_{\mathrm{RANS}}, \tilde{l}_{\mathrm{LES}}\right), \\ L_T^{(\mathrm{DX\text{-}LES})} &= l_{\mathrm{RANS}} - f_d \max\left(0, l_{\mathrm{RANS}} - l_{\mathrm{LES}}\right), \\ L_T^{(\mathrm{IDX\text{-}LES})} &= \tilde{f}_d \left(1 + f_e\right) l_{\mathrm{RANS}} + \left(1 - \tilde{f}_d\right) \hat{l}_{\mathrm{LES}}. \end{aligned}$$

3 Numerical methods

Numerical methods, described in detail in thesis, are based on finite volume method. The formulation is implicit, solving RANS Equations (1) and the turbulence model Equations (2) or (4) separately, all using the form

$$\frac{\partial \boldsymbol{W}}{\partial t} + \operatorname{div} \boldsymbol{F}_C\left(\boldsymbol{W}\right) = \operatorname{div} \boldsymbol{F}_D\left(\boldsymbol{W}\right) + \boldsymbol{Q}\left(\boldsymbol{W}\right), \tag{7}$$

where $\boldsymbol{W}$ are the conservative variables, $\boldsymbol{F}_C$ the convective fluxes, $\boldsymbol{F}_D$ the diffusive fluxes and $\boldsymbol{Q}$ the source term.

The RANS convective fluxes are approximated using the HLLC Riemann solver. Least square reconstruction with Barth-Jespersen limiter is then used to obtain $\boldsymbol{F}_C$ for both RANS and turbulence model systems of equations. The derivatives of these fluxes required by the implicit scheme are then obtained using analytical relations. For the diffuse fluxes, the gradients of variables are computed from values in points of "diamond cell".

Time discretization is done by second order backward differentiation formula (BDF2). To improve accuracy, dual time stepping is also utilized, which uses first order backward differentiation formula (BDF). The resulting linear system is then solved using the generalized minimal residual method.

The algorithm for adaptive mesh refinemet (AMR) described in the thesis is based on the refinement procedure from [17]. The level of AMR is decided based on various parameters, depending on the value of adaptation criteria. These include value of strain norm, vorticity norm, density gradient flow, deviation of local entropy from its reference value, turbulence kinetic energy and vortex identification functions from [20].

4 Results

The thesis presents various test cases, including results for the Sajben transonic converging-diverging diffuser (used by NASA to develop jet engines) from [21], which were also presented in [1]. The results shown here, however, are for tandem cylinder problem, presented in [2, 3]. This test case was used to study aircraft landing gear by NASA, which also provided experimental data in [22, 23, 24].

The tandem cylinder problem is given by two identical cylinders in a row, the first of which causing continuous vortex shedding, from which the vortex street passes to the front of the second cylinder, where the separated shear layer temporarily reattaches only to be separated again to form another vortex street.

The chosen characteristic domain length is the diameter of the cylinders $L_{\text{char}} = 0.057\,15\,\text{m}$. The cylinders have their axes $3.7L_{\text{char}}$ apart and the free stream velocity is $44\,\text{m}\,\text{s}^{-1}$. The Reynolds number is then $166,000$.

The outer boundary lies $20L_{\text{char}}$ from the surface of the cylinder and is split into two equal parts – left being for the inlet and right for the outlet BC. The cylinders inside are defined as the walls of the domain. The mesh is unstructured with $17,725$ cells in each of the 30 layers, which are $0.025D$ thick. Most of the cells are concentrated close to the cylinders or between them. The inlet turbulence intensity was chosen according to [25] as 4%.

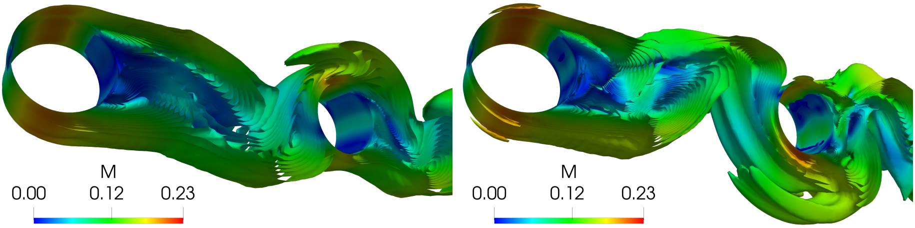

(a) TNT (b) DX-LES

Figure 1: Contours of vorticity colored by calculated Mach number obtained by the delayed DES models.

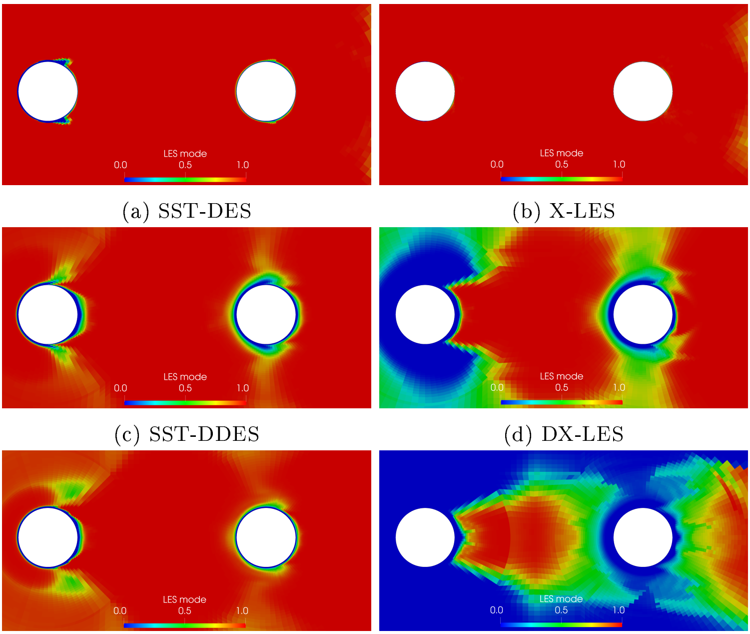

(a) SST-DES (b) X-LES

(c) SST-DDES (d) DX-LES

(e) SST-IDDES (f) IDX-LES

Figure 2: Time-averaged RANS-LES switching of different hybrid methods – value of 0 indicate RANS-only mode, while 1 is fully in LES mode.

The vorticity magnitudes colored by the Mach number at $t = 0.5\,\mathrm{s}$ are shown in Fig. 1. As expected, the base RANS methods did not show many 3D fluctuations structures and showed almost no change in the direction parallel to the cylinder axes.

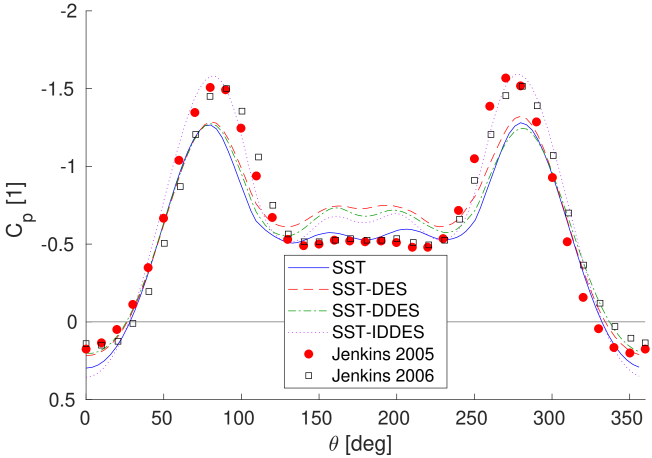

(a) SST-based models.

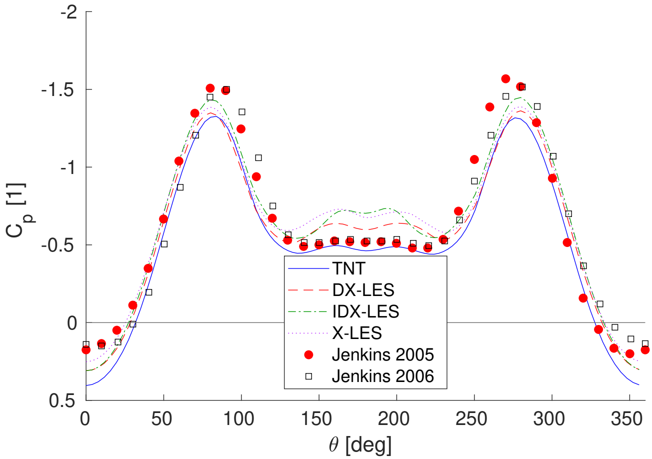

(b) TNT-based models.

Figure 3: Average pressure coefficient on the rear cylinder by the (a) SST-based and (b) TNT-based methods. Experimental data from [22, 23].

The RANS-LES switching averaged in time is shown in Fig. 2. It is interesting to note that the most simple hybrid models (SST-DES and X-LES) were in LES mode almost everywhere around the cylinders. The X-LES method was also in LES mode much closer to the walls than the SST-DES model. The DX-LES method seemed to switch into RANS mode in front of the first cylinder and even more LES-restrictive behavior showed the IDX-LES model, which switches to LES mode mostly only in areas with vortex streets.

As for the values on the walls, the values of pressure coefficient compared to the experimental data from [22, 23] are shown in Fig. 3 for the rear cylinder. The surface of the cylinders is described with the angle θ, where $\theta = 0^\circ$ denotes the front of the cylinder and $\theta = 180^\circ$ the rear. The data were averaged over outputs evenly spaced in time over several periods. Since the values of C_p should be constant behind the cylinder (in the area of separated flow), but instead show slight oscillations, it is hard to determine if these deviations are caused by imperfections in the numerical solution or if a higher sampling for the statistical evaluation would fix these results.

Results with AMR. Three types of grids were compared in this test – the base coarse mesh from the beginning of this chapter, then the dynamically adapted version of this grid and also one mesh with high resolution, which contains 78,844 cells in each layer (approximately twice as many as the average adapted grid), with cell sizes close to the wall unaltered so that the value of y^+ remains the same there. Everywhere else, however, the resolution is approximately four times that of the original mesh. This basically means that this grid corresponds to the original one with mesh adaptation applied everywhere.

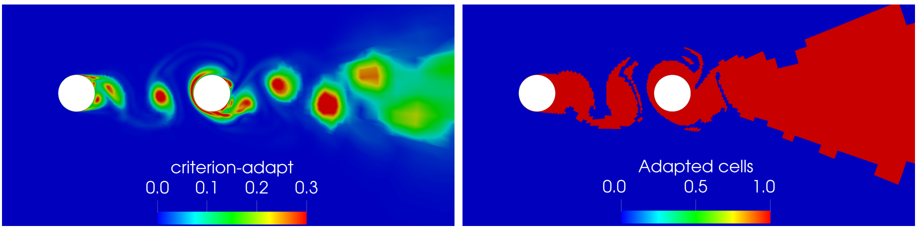

(a) Criterion values (b) Adapted cells

Figure 4: Evaluation of the entropy criterion.

The increase of resolution caused by the mesh adaptation can also allow the hybrid RANS-LES methods to switch into LES mode, which can improve results more than just a higher resolution. As seen in Fig. 5, the mesh adaptation does indeed affect the switching.

The values of pressure coefficient on the walls are shown in Fig. 6. As already seen at the beginning of this chapter in Fig. 3, the SST-DES model is the worst performing method in this test and the increased resolution did not bring any substantial improvements. However, the adapted grid seem to provide very similar results to the high resolution grid.

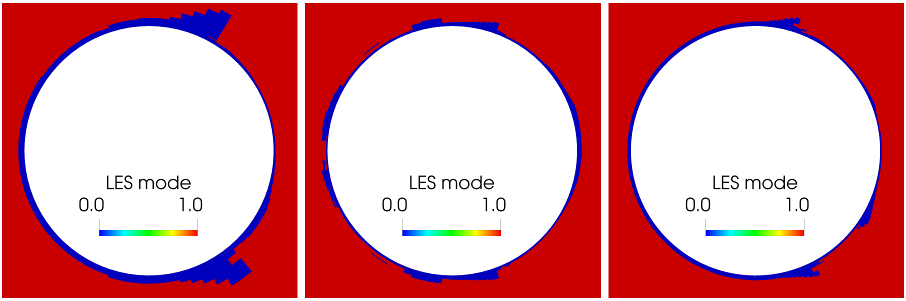

(a) Coarse grid (b) Adapted grid (c) Fine grid

Figure 5: RANS-LES switching around the front cylinder on different computational meshes using the SST-DES model – values of 0 and 1 indicate pure RANS or LES mode, respectively.

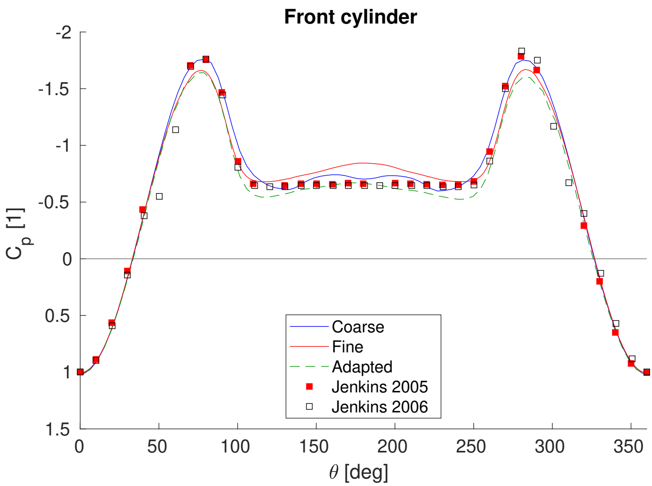

Figure 6: Average pressure coefficient calculated by the DES method on the front cylinder with different meshes.

5 Conclusions

Final Remarks and Summary of Results The objectives of the thesis have been met. The implicit formulation of the HLLC scheme in conjunction with two distinct two equation RANS and six different RANS-LES hybrid turbulence models was successfully implemented. The algorithm for adaptive mesh refinement and its criteria also seems to work as intended, as was also demonstrated.

The results show that the hybrid RANS-LES approach can bring significant improvement of the results in comparison to the base RANS methods, with minimal additional costs. The delayed models also appear to be noticeably closer to the experimental data.

The adaptive mesh refinement also affected the results of the hybrid method on the tandem cylinder problem, both in RANS-LES switching and in the quality of the results. The results on the adapted grid were in fact very close to the results obtained on the computational grid with high resolution (and approximately twice as many cells) that would have been produced by fully adapting all cells at the start of the computation, showing significant improvement over the coarse grid without any refinement.

The results overall show the usefulness of the presented hybrid RANS-LES methods as well as combining these hybrid methods with AMR. As can be seen in the results shown, with an appropriate choice of the adaptation criterion, it is possible to achieve a similar quality of results on a coarse grid as on a several times finer grid.

Research Outlook and Future Work Although the goals of the thesis have been met and the presented results can be considered successful, the work is far from over. There are several points where the investigation of hybrid RANS-LES methods and their combination with adaptation should continue:

- implement a fully 3D adaptive mesh refinement algorithm for general hybrid meshes,
- test RANS-LES hybrid methods with AMR on grids of different types, higher resolutions and higher levels of adaptation, as better hardware becomes available (as the current grid resolutions were at the limit of the hardware available at the time),
- use different hybrid methods with AMR and find more test cases.

Author's Publications

[1] L. Hájek, J. Fořt, Karel J., and Trdlička D. Comparison of Various RANS and RANS-LES Hybrid Models on a Transonic Diffuser Problem. *Topical Problems of Fluid Mechanics 2023 (D. Šimurda and T. Bodnár, eds.), Institute of Thermomechanics, AS CR*, pages 36–43, 2023.

[2] L. Hájek et al. Resolving Flow Around Tandem Cylinders with RANS-LES Hybrid Methods. *Proceedings of Computational Mechanics 2023*, pages 59–62, 2023.

[3] L. Hájek et al. Validating New RANS-LES Hybrid Methods on a Tandem Cylinder Problem [In preparation]. *Applied and Computational Mechanics.*

References

[4] P. R. Spalart, W. H. Jou, M. Strelets, and S. Allmaras. Comments on the feasibility of les for wings, and on a hybrid rans/les approach. In *Advances in DNS/LES: Direct numerical simulation and large eddy simulation*, pages 137–148, 1997.

[5] Florian Menter and M. Kuntz. *Adaptation of Eddy-Viscosity Turbulence Models to Unsteady Separated Flow Behind Vehicles*, volume 19, pages 339–352. Springer Berlin Heidelberg, Berlin, Heidelberg, 01 2004.

[6] P. Spalart, S. Deck, M. Shur, K. Squires, M. Strelets, and A. Travin. A New Version of Detached-eddy Simulation, Resistant to Ambiguous Grid Densities. *Theoretical and Computational Fluid Dynamics*, 20(3):181–195, 2006.

[7] N. V. Nikitin, F. Nicoud, B. Wasistho, K. D. Squires, and P. R. Spalart. An approach to wall modeling in large-eddy simulations. *Physics of Fluids*, 12(7):1629–1632, 2000.

[8] M. L. Shur, P. R. Spalart, M. Kh. Strelets, and A. K. Travin. A hybrid rans-les approach with delayed-des and wall-modelled les capabilities. *International Journal of Heat and Fluid Flow*, 29(6):1638–1649, 2008.

[9] M. Strelets. Detached Eddy Simulation of Massively Separated Flows. *AIAA Journal*, 2001.

[10] F. Menter. Zonal Two Equation k-ω Turbulence Models For Aerodynamic Flows. In *23rd Fluid Dynamics, Plasmadynamics, and Lasers Conference*, 1993.

[11] M. Gritskevich, A. Garbaruk, J. Schütze, and F. Menter. Development of DDES and IDDES Formulations for the k-ω Shear Stress Transport Model. *Flow, Turbulence and Combustion*, 2012.

[12] J. C. Kok, H. Dol, B. Oskam, and H. van der Ven. Extra-large-eddy simulation of massively separated flows. In *42nd AIAA Aerospace Sciences Meeting and Exhibit*, 2004.

[13] J. C. Kok. Resolving the dependence on freestream values for $k - \omega$ turbulence model. *Notes on Numerical Fluid Mechanics and Multidisciplinary Design, Springer*, 38(7):1292–1295, 2007.

[14] J. C. Kok and H. van der Ven. Destabilizing Free Shear Layers in X-LES Using a Stochastic Subgrid-Scale Model. *National Aerospace Laboratory NLR, report no. NLR-TP-2009-327*, 2009.

[15] A. Fracassi, R. De Donno, A. Ghidoni, and G. Noventa. Implementation and Validation of the SST Delayed eXtra-LES Model for Complex Turbulent Flows. *International Journal of Computational Fluid Dynamics*, 36:1–24, 2022.

[16] S. Mozaffari, E. Guilmineau, M. Visonneau, and J. Wackers. Average-based mesh adaptation for hybrid RANS/LES simulation of complex flows. *Computers and Fluids*, 232, 2022.

[17] J. Karel. Numerical Simulation of Streamer Propagation on Unstructured Dynamically Adapted Grids. *Doctoral Thesis, Czech Technical University in Prague and Université Paris 13*, 2014.

[18] Christopher Rumsey. Implementing Turbulence Models into the Compressible RANS Equations. `https://turbmodels.larc.nasa.gov/implementrans.html`, accessed 2023.

[19] F. Menter, M. Kuntz, and R. B. Langtry. Ten years of industrial experience with the SST turbulence model. *Heat and Mass Transfer*, 4, 2003.

[20] L. Graftieaux, M. Michard, and N. Grosjean. Combining PIV, POD and Vortex Identification Algorithms for the Study of Unsteady Turbulent Swirling Flows. *Measurement Science and Technology*, 12(9), 2001.

[21] J. W. Slater. NPARC Alliance Verification and Validation Archive. `https://www.grc.nasa.gov/www/wind/valid/archive.html`, accessed 2022.

[22] L. Jenkins, M. Khorrami, M. Choudhari, and C. McGinley. Characterization of unsteady flow structures around tandem cylinders for component interaction studies in airframe noise. In *11th AIAA/CEAS Aeroacoustics Conference*, 2005.

[23] L. Jenkins, D. Neuhart, C. McGinley, M. Khorrami, and M. Choudhari. Measurements of unsteady wake interference between tandem cylinders. In *36th AIAA fluid dynamics conference and exhibit*, 2006.

[24] M. Khorrami, M. Choudhari, D. Lockard, L. Jenkins, and C. McGinley. Unsteady flowfield around tandem cylinders as prototype component interaction in airframe noise. *Aiaa Journal - AIAA J*, 45:1930–1941, 2007.

[25] R. Maduta, M. Ullrich, and S. Jakirlic. Reynolds stress modelling of wake interference of two cylinders in tandem: Conventional vs. eddy-resolving closure. *International Journal of Heat and Fluid Flow*, 67:139–148, 2017. Symposium on Experiments and Simulations in Fluid Dynamics Research.

Summary

This thesis deals with turbulence modeling methods based on two different approaches – the Reynolds-averaged Navier–Stokes (RANS) equations and large eddy simulation (LES). These hybrid methods came into existence to combine the lower computational demands of RANS and the eddy modeling ability of LES. Six different RANS-LES hybrid methods based on two different RANS methods are described and used in this thesis, two of which are newly proposed as part of this work. The mathematical model is then numerically approximated using an implicit finite volume method formulation and implemented in the in-house software Orion using parallel computing techniques with the help of the PETSc numerical library.

The switching between RANS and LES is affected by the turbulent quantities and cell size in the computational mesh, so it is natural to adjust its resolution to control which mode should be used. This is the reason why this thesis proposes to use adaptive mesh refinement (AMR) with these hybrid methods. To determine in which part of the computational domain should AMR be utilized, several criteria to quickly detect turbulence phenomena like vortices are proposed. The computational mesh is then refined in these selected regions to improve both the grid resolution in important areas and RANS-LES switching.

The implemented hybrid models with various RANS-LES switching methods are then tested and compared with each other, their RANS counterparts and also real experimental data. Solved problems include a diffuser, vortex shedding behind a cylinder at low Reynolds number and vortex shedding behind tandem cylinders at high Reynolds number. These just mentioned problems play an important role in the development of jet engines and aircraft landing gear.

The presented results show the usefulness of the hybrid methods over the base RANS models, differences between various RANS-LES switching techniques and also the benefits of using adaptive mesh refinement with a suitable criterion instead of increasing the mesh resolution en masse right away.

Keywords: Computational fluid dynamics, turbulence modeling, finite volume method, implicit scheme, Orion software, RANS-LES hybrid methods, detached eddy simulation, adaptive mesh refinement, vortex shedding

Resumé

Tato práce se zabývá metodami modelování turbulentního proudění založenými na dvou rozdílných přístupech – reynoldsovsky vystředovaných Navierových–Stokesových (RANS) rovnicích a metodě simulace velkých vírů (LES). Takovéto hybridní modely vznikly za účelem spojení výhod obou přístupů, tedy nižší výpočetní náročnosti RANS metod a schopnosti zachytit víry LES metod. Šest různých hybridních RANS-LES modelů založených na dvou jiných RANS metodách je popsáno a použito v této práci, z toho dvě byly nově navrženy v rámci této dizertace. Matematický model je poté numericky aproximován pomocí implicitní formulace metody konečných objemů a jako paralelizovaný algoritmus implementován v in-house výpočetním softwaru Orion za využití numerické knihovny PETSc.

Přepínání mezi RANS a LES je ovlivněno turbulentními veličinami a velikostí buněk výpočetní sítě, takže je přirozené její rozlišení upravovat za účelem ovlivnění tohoto přepínání. To je důvodem k tomu, proč tato práce navrhuje použití adaptivního zjemnění sítě v kombinaci s těmito hybridními metodami. Pro určení toho, ve které části výpočetní domény by měla být adaptace sítě využita, je navrženo několik kritérií k rychlé detekci turbulentních jevů (např. vírů). Výpočetní sít je pak zjemněna v těchto vybraných oblastech, aby bylo dosaženo nejen lepšího rozlišení v důležitých místech, ale také lepšího RANS-LES přepínání.

Implementované hybridní metody s různými metodami RANS-LES přepínání jsou následně testovány a porovnávány jak mezi sebou, tak i se svými základními RANS modely i reálnými experimenty. Mezi řešenými úlohami je difuzor, nestacionární proudění kolem válce při nízkém Reynoldsově čísle a neustálené trhání proudu dvěma válcovými tyčemi za sebou při vysokém Reynoldsově čísle. Tyto zmíněné případy hrají důležitou roli například pro vývoj proudových motorů a podvozků letadel.

Výsledky v této práci ukazují přednosti hybridních metod oproti základním RANS modelům, rozdíly mezi různými metodami RANS-LES přepínání a také výhody použití adaptivního zjemnění sítě s vhodným kritériem namísto zvyšování rozlišení sítě hromadně ještě před začátkem výpočtu.

Klíčová slova: Výpočetní dynamika tekutin, modelování turbulence, metoda konečných objemů, implicitní schéma, software Orion, hybridní metody RANS-LES, metody DES, adaptivní zjemnění sítě